

A C^0P_2 TIME-STEPPING VIRTUAL ELEMENT METHOD FOR LINEAR WAVE EQUATIONS ON POLYGONAL MESHES

JIANGUO HUANG* AND SEN LIN

School of Mathematical Science, and MOE-LSC
Shanghai Jiao Tong University
Shanghai 200240, China

ABSTRACT. This paper is concerned with a C^0P_2 time-stepping virtual element method (VEM) for solving linear wave equations on polygonal meshes. The spatial discretization is carried out by the VEM while the temporal discretization is obtained based on the C^0P_2 time-stepping approach, leading to a fully discrete method. The error estimates in the H^1 semi-norm and L^2 norm are derived after detailed derivation. Finally, the numerical performance and efficiency of the proposed method is illustrated by several numerical experiments.

1. Introduction. In the past few years, a new numerical method called the virtual element method (VEM) has received much attention in the field of scientific computing. The pioneering works can be found in [3, 2, 5, 11]. VEMs can be regarded as a generalization of usual finite element methods that can easily handle polytopal meshes, which have several significant advantages over standard finite element methods, such as (1) they are convenient for solving problems on complex geometric domains; (2) they are suitable for attacking problems associated with high regularity admissible spaces (see [8]). Until now, such methods have been used to solve a variety of mathematical physical problems. We refer to [4, 7, 9, 13, 14, 17, 18, 19, 20, 23, 27, 28, 29, 30, 31] and references therein for details about their applications for steady variational problems in primal formulations.

However, there are few works on unsteady problems using VEMs. Some relevant results can be found in [27, 28]. In [28], after temporal discretization by the usual backward Euler method and spatial discretization by the VEM in [2], a fully discrete method was proposed and analyzed for linear parabolic equations. Similar ideas were further extended to handle linear wave equations in [27] with the focus on discussing the semidiscrete method. A fully discrete method is developed by the Newmark method and the Bathe method for temporal discretization, and the error analysis is studied briefly. It is remarked that all these methods are equal-sized in time direction. In this paper, we are devoted to proposing a fully discrete method for linear wave equations with the temporal discretization carried out by the C^0 -continuous time-stepping methods as used in [21, 22] while the spatial discretization

2020 *Mathematics Subject Classification.* Primary: 65M60, 65M15; Secondary: 35L20.

Key words and phrases. Virtual element method, C^0P_2 time-stepping, linear wave equations, polygonal meshes, error analysis.

The work was partially supported by NSFC (Grant No. 11571237).

* Corresponding author: jghuang@sjtu.edu.cn.

by the VEM in [2], respectively. We develop optimal error estimates in the H^1 semi-norm and L^2 norm by using the energy method, which are equal to $O(h^k + \tau^3)$ and $O(h^{k+1} + \tau^3)$, respectively, where h and τ denote respectively the mesh sizes in space and time, and k denotes the order of the VEM approximation. Our method can use a non-uniform subdivision in time, more flexible in numerically solving linear wave equations. We also offer several numerical experiments to illustrate the performance of the proposed method. Moreover, the numerical comparison indicates that our method proposed performs better than the one in [27] in accuracy.

The rest of this paper is organized as follows. In Section 2, we introduce the model continuous problem and present the VEM semi-discrete method. In Section 3, we propose the C^0P_2 time-stepping VEM. Some fundamental results are given in Section 4, followed by error estimates for the method in Section 5. Finally we present some numerical tests in Section 6 to show the performance of the method proposed.

2. The continuous and discrete problems.

2.1. The continuous problem. Let $\Omega \subset \mathbb{R}^2$ be a polygonal domain of interest. The linear wave equation can be described as

$$\begin{cases} u_{tt} - \Delta u = f & \text{in } \Omega \times I, \\ u = 0 & \text{on } \partial\Omega \times I, \\ u(\cdot, 0) = \Psi_0, \quad u_t(\cdot, 0) = \Psi_1 & \text{in } \Omega, \end{cases} \quad (2.1)$$

where $I := (0, T)$, u represents the unknown function to be sought, u_t and u_{tt} denote respectively its first and second order time derivative. Assume the source term $f \in L^2(\Omega \times I)$ and the initial data $\Psi_0, \Psi_1 \in H_0^1(\Omega)$.

Then the variational formulation of the problem (2.1) reads

$$\begin{cases} \text{find } u \in C^0(0, T; H_0^1(\Omega)) \cap C^1(0, T; L^2(\Omega)), \text{ such that} \\ (u_{tt}(t), v) + a(u(t), v) = (f(t), v) \quad \forall v \in H_0^1(\Omega), \text{ for a.e. } t \text{ in } (0, T), \\ u(0) = \Psi_0, \quad u_t(0) = \Psi_1, \end{cases} \quad (2.2)$$

where (\cdot, \cdot) denotes the $L^2(\Omega)$ inner product, $a(u, v) := (\nabla u, \nabla v)$ for u and v in $H_0^1(\Omega)$, and the partial derivative u_{tt} should be understood in the sense of distribution with respect to t .

Define the $H^1(\Omega)$ semi-norm via $|v|_1^2 = a(v, v)$, which is actually a norm on $H_0^1(\Omega)$ by the Poincaré-Friedrichs inequality and is equivalent to the usual $H^1(\Omega)$ norm. The bilinear form $a(\cdot, \cdot)$ is continuous and coercive, i.e. there exist two uniform positive constants M and α such that

$$a(u, v) \leq M|u|_1|v|_1, \quad a(v, v) \geq \alpha|v|_1^2 \quad \forall u, v \in H_0^1(\Omega).$$

As shown in [24, 27], Problem (2.2) has a unique solution $u(t)$ satisfying

$$\left(a(u(t), u(t)) + \|u_t(t)\|_{L^2(\Omega)}^2 \right)^{1/2} \leq \left(a(\Psi_0, \Psi_0) + \|\Psi_1\|_{L^2(\Omega)}^2 \right)^{1/2} + \|f\|_{L^1(0,t; L^2(\Omega))}$$

for all t in $(0, T)$.

Next, introduce some notation for later requirements. As in [1, 10], given a bounded domain D in \mathbb{R}^d ($d = 1, 2$) and a non-negative integer s , denote by $H^s(D)$

the standard Sobolev spaces with the following norm and seminorm:

$$\|v\|_{s,D} = \left(\sum_{|\beta| \leq s} \int_D |\partial^\beta v|^2 dx \right)^{1/2}, \quad |v|_{s,D} = \left(\sum_{|\beta|=s} \int_D |\partial^\beta v|^2 dx \right)^{1/2} \quad \forall v \in H^s(D).$$

Moreover, denote by $(\cdot, \cdot)_\omega$ the L^2 scalar product on an open subset $\omega \subseteq D$.

Let B be a Banach space equipped with the norm $\|\cdot\|_B$. For $1 \leq p \leq \infty$, define

$$L^p(0, T; B) = \{v : [0, T] \rightarrow B \text{ is Lebesgue measurable; } \|v\|_{L^p(0,T;B)} < \infty\},$$

where

$$\|v\|_{L^p(0,T;B)} := \left(\int_0^T \|v(\cdot, t)\|_B^p dt \right)^{1/p}, \quad 1 \leq p < \infty,$$

and

$$\|v\|_{L^\infty(0,T;B)} := \text{esssup}_{0 \leq t \leq T} \|v(\cdot, t)\|_B.$$

We also define

$$H^s(0, T; B) = \{v : [0, T] \rightarrow B \text{ is Lebesgue measurable; } \|\partial_t^m v\|_{L^2(0,T;B)} < \infty, \quad 0 \leq m \leq s\},$$

equipped with the norm

$$\|v\|_{H^s(0,T;B)} = \left(\sum_{0 \leq m \leq s} \|\partial_t^m v\|_{L^2(0,T;B)}^2 \right)^{1/2}.$$

To simplify the presentation, write

$$\|v\|_{s,D} = \|v(\cdot, t)\|_{s,D}, \quad |v|_{\infty,s} = \text{esssup}_{0 \leq t \leq T} |v(\cdot, t)|_{s,\Omega}.$$

In our forthcoming analysis, the symbol C stands for a generic positive constant independent of the mesh size h and the time step size τ , which may take different values at different occurrences. And for any two quantities a and b , $a \lesssim b$ indicates $a \leq Cb$.

2.2. The virtual semi-discrete method. Let $\{\mathcal{T}_h\}_h$ be a family of conforming partitions of Ω into general polygonal polygons E , and

$$h_E := \text{diameter}(E), \quad h := \sup_{E \in \mathcal{T}_h} h_E.$$

For each polygonal element E with n_E edges, denote by $\{P_i\}_{i=1}^{n_E}$ its vertices which are numbered in a counter-clockwise order and by e_i the edge connecting P_i and P_{i+1} , where we identify P_{n_E+1} as P_1 . The dependence on E will be always omitted when no confusion can arise. In this subsection, we will obtain the VEM semi-discrete problem based on the VEM given in [28, 27], with the family of polygonal meshes $\{\mathcal{T}_h\}_h$ satisfying the following condition (cf. [12, 16]):

- A1.** For each $E \in \mathcal{T}_h$, there exists a “virtual triangulation” \mathcal{T}_E of E such that \mathcal{T}_E is uniformly shape regular and quasi-uniform. The corresponding mesh size of \mathcal{T}_E is proportional to h_E . Each edge of E is a side of a certain triangle in \mathcal{T}_E .

As shown in [16], this condition covers the usual geometric assumptions frequently used in the context of VEMs.

We will adopt two main steps to get the virtual element discretization of Problem (2.2). Firstly, we consider how to construct the local virtual element space and the local discrete bilinear form on each element E . Then we obtain the global virtual element space and the global discrete bilinear form based on their local counterparts.

For all natural number $k \geq 1$ and $E \in \mathcal{T}_h$, introduce the following function spaces:

- $\mathbb{P}_k(E)$ is the set of all polynomials on E with the total degree no more than k ;
- $\mathbb{B}_k(\partial E) := \{v \in C^0(\partial E); v|_e \in \mathbb{P}_k(e) \ \forall e \subset \partial E\}$,

where conventionally $\mathbb{P}_{-1}(E) = \{0\}$.

For a broken Sobolev space $H^1(\mathcal{T}_h) := \Pi_{E \in \mathcal{T}_h} H^1(E)$, define a broken H^1 semi-norm by

$$|v|_{h,1} = \left(\sum_{E \in \mathcal{T}_h} |\nabla v|_{0,E}^2 \right)^{1/2}.$$

For all $E \in \mathcal{T}_h$, introduce an augmented local virtual element space $\tilde{V}_k(E)$ by

$$\tilde{V}_k(E) = \{v \in H^1(E); v \in \mathbb{B}_k(\partial E), \Delta v \in \mathbb{P}_k(E)\}.$$

Then define a local modified virtual element space $W_k(E)$ (which is isomorphic to $\tilde{V}_k(E)$) as

$$W_k(E) = \left\{ w \in \tilde{V}_k(E); (w - \Pi_k^{\nabla,E} w, q^*)_E = 0 \ \forall q^* \in \mathbb{M}_k(E)/\mathbb{M}_{k-2}(E) \right\}, \quad (2.3)$$

where $\Pi_k^{\nabla,E}$ stands for the H^1 -projection to $\mathbb{P}_k(E)$, defined later in this subsection, and $\mathbb{M}_\ell(D)$ denotes the scaled monomial on a d -dimensional domain D , i.e.

$$\mathbb{M}_\ell(D) := \{(\mathbf{x} - \mathbf{x}_D)^{\mathbf{s}} / h_D^{|\mathbf{s}|}, \quad |\mathbf{s}| \leq \ell\},$$

with \mathbf{x}_D the barycenter of D , h_D the diameter of D or $h_D = |D|^{1/d}$, and ℓ a non-negative integer.

Next, we consider the dual space $\mathcal{X}_k(E)$ of $W_k(E)$ defined as

$$\mathcal{X}_k(E) = \text{span}\{ \chi_v, \chi_e^{k-2}, \chi_E^{k-2} \},$$

where the functional vectors $\chi_v, \chi_e^{k-2}, \chi_E^{k-2}$ are obtained via introducing the following set of linear functionals of $W_k(E)$. For all $v \in W_k(E)$ we take (see Figure 1):

- χ_v : Values of v at the n_E internal vertices.
- χ_e^{k-2} : All moments on edges of E up to order $k-2$, i.e.

$$\chi_e(v) = |e|^{-1} (m, v)_e \ \forall m \in \mathbb{M}_{k-2}(e), \ \forall e \subset \partial E$$

(alternatively, we can also choose the function values at the $k-1$ internal points of the $(k+1)$ -Gauss-Lobatto quadrature rule in e , as suggested in [5]).

- χ_E^{k-2} : All moments on elements E up to order $k-2$, i.e.

$$\chi_E(v) = |E|^{-1} (m, v)_E \ \forall m \in \mathbb{M}_{k-2}(E).$$

As shown in [3, 6], the set of degrees of freedom (d.o.f.s) given above are unisolvent for $W_k(E)$, i.e. $(W_k(E))' = \mathcal{X}_k(E)$. So the triple $(E, W_k(E), \mathcal{X}_k(E))$ really forms a finite element. Relabel the d.o.f.s by a single index $i = 1, 2, \dots, n_{\text{dof}} := \dim W_k(E)$. Therefore, with these d.o.f.s we can associate a canonical basis $\{\phi_1, \phi_2, \dots, \phi_{n_{\text{dof}}}\}$ of $W_k(E)$ such that

$$\chi_i(\phi_j) = \delta_{ij}, \quad i, j = 1, 2, \dots, n_{\text{dof}}.$$

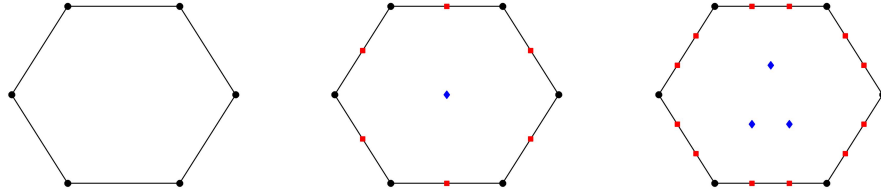


FIGURE 1. Degrees of freedom for $k = 1, 2, 3$. Denote χ_v with black dots, χ_e^{k-2} with red squares, and χ_E^{k-2} with blue diamonds.

The basis $\{\phi_j\}_{j=1}^{n_{\text{dof}}}$ do not need to be written explicitly and this is the reason of the word “virtual” in VEM. Then every function $v \in W_k(E)$ can be expanded as

$$v(x) = \sum_{i=1}^{n_{\text{dof}}} \chi_i(v) \phi_i(x)$$

and in numerical computation it can be identified as a vector $\mathbf{v} \in \mathbb{R}^{n_{\text{dof}}}$ in the form

$$\mathbf{v} = (\chi_1(v), \chi_2(v), \dots, \chi_{n_{\text{dof}}}(v))^{\mathbf{T}}.$$

Thus we can establish an isomorphism between functions in $W_k(E)$ and vectors in $\mathbb{R}^{n_{\text{dof}}}$:

$$\chi : W_k(E) \rightarrow \mathbb{R}^{n_{\text{dof}}}, \quad \chi(v) = (\chi_1(v), \chi_2(v), \dots, \chi_{n_{\text{dof}}}(v))^{\mathbf{T}}.$$

Next, define the local H^1 projection operator: $\Pi_k^{\nabla,E} : H^1(E) \rightarrow \mathbb{P}_k(E)$ as the solution of

$$\begin{cases} (\nabla(\Pi_k^{\nabla,E} v), \nabla q_k)_E = (\nabla v, \nabla q_k)_E \quad \forall q_k \in \mathbb{P}_k(E), \\ P^{0,E}(v - \Pi_k^{\nabla,E} v) = 0, \end{cases} \quad (2.4)$$

where $P^{0,E} : H^1(E) \rightarrow \mathbb{R}$ is taken as

$$\begin{cases} P^{0,E}(v) := \frac{1}{|\partial E|} \int_{\partial E} v \, ds & \text{for } k = 1, \\ P^{0,E}(v) := \frac{1}{|E|} \int_E v \, dx & \text{for } k > 1. \end{cases}$$

In order to handle the time term $(u_{tt}(t), v)$ in (2.2), we also introduce the local $L^2(E)$ projection operator $\Pi_k^{0,E}$ from $L^2(E)$ to $\mathbb{P}_k(E)$, defined by

$$(\Pi_k^{0,E} v, q_k)_E = (v, q_k)_E \quad \forall q_k \in \mathbb{P}_k(E). \quad (2.5)$$

As in [2], we conclude that $\Pi_k^{\nabla,E} = \Pi_k^{0,E}$ for the case $k \leq 2$.

Using an integration by parts, the right hand side of the first equation of (2.4) can be written as

$$(\nabla v, \nabla q_k)_E = -(v, \Delta q_k)_E + \langle v, \nabla q_k \cdot \mathbf{n} \rangle_{\partial E},$$

therefore $\Pi_k^{\nabla,E} v$ is computable with the d.o.f.s of $v \in W_k(E)$. So is the quantity $\Pi_k^{0,E} v$.

Since for all $u_h, v_h \in W_k(E)$, the quantities $a^E(u_h, v_h) := (\nabla u_h, \nabla v_h)_E$ and $(u_h, v_h)_E$ are not computable, we should modify the two local bilinear forms accordingly. So we define two bilinear forms $a_h^E(\cdot, \cdot)$ and $m_h^E(\cdot, \cdot)$ such that

$$\begin{aligned} a_h^E(\cdot, \cdot) &: W_k(E) \times W_k(E) \rightarrow \mathbb{R}, \\ m_h^E(\cdot, \cdot) &: W_k(E) \times W_k(E) \rightarrow \mathbb{R} \end{aligned}$$

to approximate the previous bilinear forms.

Note that $a^E(\Pi_k^{\nabla, E} u, \Pi_k^{\nabla, E} v)$ (resp. $(\Pi_k^{0, E} u, \Pi_k^{0, E} v)_E$) alone does not lead to a stable method, a stabilization term $\mathcal{S}^E(\cdot, \cdot)$ (resp. $\mathcal{R}^E(\cdot, \cdot)$) should be added to overcome the difficulty. To ensure the stability while maintaining the accuracy, we should impose the following assumptions on the element-wise stabilization terms $\mathcal{R}^E(\cdot, \cdot)$ and $\mathcal{S}^E(\cdot, \cdot)$ (cf. [3]).

- **k-consistency:** For all $q \in \mathbb{P}_k(E)$ and $v \in W_k(E)$,

$$\mathcal{S}^E(q, v) = 0, \quad \mathcal{R}^E(q, v) = 0.$$

- **Stability:** There exist positive constants α_* , α^* independent of h and E , such that, for all $\tilde{v} \in (I - \Pi_k^{\nabla, E})W_k(E)$, there holds

$$\begin{aligned} \alpha_* a^E(\tilde{v}, \tilde{v}) &\leq \mathcal{S}^E(\tilde{v}, \tilde{v}) \leq \alpha^* a^E(\tilde{v}, \tilde{v}), \\ \alpha_* (\tilde{v}, \tilde{v})_E &\leq \mathcal{R}^E(\tilde{v}, \tilde{v}) \leq \alpha^* (\tilde{v}, \tilde{v})_E. \end{aligned}$$

Then following the VEM framework, for all u and v in $W_k(E)$, define

$$a_h^E(u, v) = a^E(\Pi_k^{\nabla, E} u, \Pi_k^{\nabla, E} v) + \mathcal{S}^E((I - \Pi_k^{\nabla, E})u, (I - \Pi_k^{\nabla, E})v), \quad (2.6)$$

$$m_h^E(u, v) = (\Pi_k^{0, E} u, \Pi_k^{0, E} v)_E + \mathcal{R}^E((I - \Pi_k^{0, E})u, (I - \Pi_k^{0, E})v). \quad (2.7)$$

Remark 1. VEMs are in fact a family of schemes different in the choice of the stabilization terms. For our problem discussed here, one of the key points is the construction of $\mathcal{S}^E(\cdot, \cdot)$ and $\mathcal{R}^E(\cdot, \cdot)$. The typical choice for the two terms was given in [2, 3, 5], which is also suitable under the geometric assumption **A1** by using the norm equivalence given in [16]. Concretely speaking, for all u and v in $W_k(E)$,

$$\mathcal{S}^E(u, v) := \sum_{i=1}^{n_{\text{dof}}} \chi_i(u - \Pi_k^{0, E} u) \chi_i(v - \Pi_k^{0, E} v) = \chi(u - \Pi_k^{0, E} u) \cdot \chi(v - \Pi_k^{0, E} v),$$

$$\mathcal{R}^E(u, v) := h_E^2 \sum_{i=1}^{n_{\text{dof}}} \chi_i(u - \Pi_k^{0, E} u) \chi_i(v - \Pi_k^{0, E} v) = h_E^2 \chi(u - \Pi_k^{0, E} u) \cdot \chi(v - \Pi_k^{0, E} v).$$

Now we define the global virtual element space by assembling the set of local spaces $W_k(E)$, described as

$$W_h = \{w \in H_0^1(\Omega); w|_E \in W_k(E) \quad \forall E \in \mathcal{T}_h\}, \quad (2.8)$$

and its dimension is

$$\dim(W_h) = N_V + (k-1)N_e + N_P \frac{k(k-1)}{2} \equiv N_{\text{dof}},$$

where N_P (resp. N_V and N_e) is the number of elements (resp. internal vertexes and edges) in \mathcal{T}_h , and N_{dof} the number of degrees of freedom of W_h . The global degrees of freedom for W_h are chosen as follows.

- **G1:** Values of v at the n_E vertexes of the polygon E .
- **G2:** Values of v at the $k-1$ internal points of the $(k+1)$ -Gauss-Lobatto quadrature rule on e .

- **G3:** All moments up to order $k - 2$ of v on each element E .

Also, define the global approximated bilinear forms $a_h(\cdot, \cdot) : W_h \times W_h \rightarrow \mathbb{R}$ and $m_h(\cdot, \cdot) : W_h \times W_h \rightarrow \mathbb{R}$ via summing the local counterparts:

$$a_h(u, v) = \sum_{E \in \mathcal{T}_h} a_h^E(u, v) \quad \forall u, v \in W_h, \tag{2.9}$$

$$m_h(u, v) = \sum_{E \in \mathcal{T}_h} m_h^E(u, v) \quad \forall u, v \in W_h. \tag{2.10}$$

It is evident that

$$a_h(u, v) \lesssim |u|_1 |v|_1, \quad m_h(u, v) \lesssim \|u\|_0 \|v\|_0 \quad \forall u, v \in W_h.$$

Thus we introduce the approximated H^1 semi-norm and the approximated L^2 norm by

$$|v|_{1,h}^2 := a_h(v, v), \quad \|v\|_{0,h}^2 := m_h(v, v) \quad \forall v \in W_h. \tag{2.11}$$

By means of $\Pi_k^{0,E}$, we define the approximated source term $f_h(t)$ for all $t \in (0, T)$ as

$$f_h(t) := \Pi_k^{0,E} f(t) \quad \forall E \in \mathcal{T}_h. \tag{2.12}$$

Thus we can construct a computable approximation $(f_h(t), v)$ for the right-hand side (f, v) in (2.2).

As usual, in order to impose the computable initial conditions, introduce the modified H^1 projection $\mathcal{P}^\nabla : H_0^1(\Omega) \rightarrow W_h$ defined by

$$\begin{cases} \text{find } \mathcal{P}^\nabla u \in W_h \text{ for } u \in H_0^1(\Omega) \text{ such that} \\ a_h(\mathcal{P}^\nabla u, v_h) = a(u, v_h) \quad \forall v_h \in W_h. \end{cases} \tag{2.13}$$

Then the suitable discrete initial data $\Psi_{0,h}$ and $\Psi_{1,h}$ can be chosen as

$$\begin{cases} \text{find } \Psi_{0,h} := \mathcal{P}^\nabla \Psi_0, \Psi_{1,h} := \mathcal{P}^\nabla \Psi_1 \text{ respectively such that} \\ a_h(\mathcal{P}^\nabla \Psi_0, v_h) = a(\Psi_0, v_h) \quad \text{and} \\ a_h(\mathcal{P}^\nabla \Psi_1, v_h) = a(\Psi_1, v_h) \quad \forall v_h \in W_h. \end{cases} \tag{2.14}$$

According to (2.8), (2.9), (2.10), (2.12) and (2.14), we are ready to construct the virtual semi-discrete approximation to Problem (2.2) as follows.

$$\begin{cases} \text{Find } u_h \in C^0(0, T; W_h) \cap C^1(0, T; W_h) \text{ such that} \\ m_h(u_{h,tt}(t), v_h) + a_h(u_h(t), v_h) = (f_h(t), v_h) \quad \forall v_h \in W_h, \text{ for a.e. } t \text{ in } (0, T), \\ u_h(0) = \Psi_{0,h}, \quad u_{h,t}(0) = \Psi_{1,h}. \end{cases} \tag{2.15}$$

Remark 2. Different from the finite element method, we should use $m_h(u_{h,tt}(t), v_h)$ instead of $(u_{h,tt}(t), v_h)$, since the latter one is not computable.

For developing error analysis later on, we also introduce the L^2 -projection operator $\mathcal{P}^0 : L^2(\Omega) \rightarrow W_h$ defined by

$$\begin{cases} \text{find } \mathcal{P}^0 u \in W_h \text{ for } u \in L^2(\Omega) \text{ such that} \\ m_h(\mathcal{P}^0 u, v_h) = (u, v_h)_{L^2(\Omega)} \quad \forall v_h \in W_h. \end{cases} \tag{2.16}$$

Referring to [28, 27], the following approximation results hold.

Lemma 2.1. For all $u \in H_0^1(\Omega) \cap H^{k+1}(\Omega)$, there holds

$$|\mathcal{P}^\nabla u - u|_{1,\Omega} \lesssim h^k |u|_{k+1,\Omega}. \quad (2.17)$$

Furthermore, if the domain Ω is convex, we have

$$\|\mathcal{P}^\nabla u - u\|_{0,\Omega} \lesssim h^{k+1} |u|_{k+1,\Omega}. \quad (2.18)$$

Lemma 2.2. If $u \in H^{k+1}(\Omega)$, there holds

$$\|\mathcal{P}^0 u - u\|_{0,\Omega} \lesssim h^{k+1} |u|_{k+1,\Omega}. \quad (2.19)$$

3. The $C^0 P_2$ time-stepping VEM. Consider a non-uniform subdivision for the time interval I with the nodes: $0 = t_0 < t_1 < \dots < t_N = T$. For $0 \leq n \leq N-1$, write $I_n := (t_n, t_{n+1})$ with time length $\tau_n = t_{n+1} - t_n$, $\tau := \max_{0 \leq n \leq N-1} \tau_n$, and introduce the following notation:

$$v^n = v(t_n) = v(x, t_n), \quad v_\pm^n(x) = \lim_{\delta \rightarrow 0^+} v(x, t_n \pm \delta), \quad [v]_n = v_+^n - v_-^n.$$

Now, we define the space-time discrete space by

$$S^{h\tau} = \{v_h : [0, T] \rightarrow W_h; v_h \in C(\bar{I}), v_h|_{I_n} = \sum_{j=0}^2 v_{h,j} t^j, \quad (3.1)$$

$$v_{h,j} \in W_h, 0 \leq n \leq N-1\},$$

and denote by $S_n^{h\tau}$ the restriction of $S^{h\tau}$ to I_n .

Based on (2.15) and following some ideas in [21], we propose a space-time virtual element scheme for Problem (2.1) as follows.

$$\begin{cases} \text{Find } U \in S^{h\tau} \text{ such that for } n = 0, 1, \dots, N-1 \\ \int_{I_n} (m_h(\ddot{U}, \dot{v}) + a_h(U, \dot{v})) dt + m_h([\dot{U}]_n, \dot{v}_+^n) = \int_{I_n} (f_h(t), \dot{v}) dt \quad \forall v \in S_n^{h\tau}, \\ U^0 = \Psi_{0,h}, \quad \dot{U}_-^0 = \Psi_{1,h}, \end{cases} \quad (3.2)$$

where $m_h(\cdot, \cdot)$ and $a_h(\cdot, \cdot)$ are defined in (2.10) and (2.9), respectively. Here, we also use the notation $\dot{v} := v_t = \partial v / \partial t$ and $\ddot{v} := v_{tt} = \partial^2 v / \partial t^2$.

We call the scheme (3.2) as the $C^0 P_2$ time-stepping VEM. Next, we present the numerical implementation method (3.2). We know $U \in S^{h\tau}$ is continuous at $t = t_n$ and is a second order polynomial in the variable t on the subinterval I_n , so $U|_{I_n}$ is uniquely determined by U^n , U^{n+1} and \dot{U}_+^n . Hence, by some direct computation, for $t \in (t_n, t_{n+1})$, the function U and \dot{U} can be expressed as

$$U(t) = \frac{1}{\tau_n^2} [(- (t - t_n)^2 + (t_{n+1} - t_n)^2) U^n + (t - t_n)^2 U^{n+1} - \tau_n (t - t_n)(t - t_{n+1}) \dot{U}_+^n], \quad (3.3)$$

$$\dot{U}(t) = \frac{1}{\tau_n^2} [-2(t - t_n) U^n + 2(t - t_n) U^{n+1} - \tau_n (2t - t_n - t_{n+1}) \dot{U}_+^n]. \quad (3.4)$$

By (3.4), we have

$$\ddot{U}(t) = \frac{2}{\tau_n^2} (-U^n + U^{n+1} - \tau_n \dot{U}_+^n).$$

Then inserting (3.3) and (3.4) into the first equation of (3.2) and taking \dot{v} to be ϕ and $(t - t_n)\eta$ respectively on I_n where $\phi, \eta \in W_h$, we are able to derive the explicit formulation for the full discrete scheme (3.2), i.e. the following linear system:

Find $\{U\}_{n=0}^N$ and $\{\dot{U}_+^n\}_{n=0}^{N-1}$ in W_h such that

$$\begin{cases} \frac{2}{\tau_n}m_h(U^{n+1}, \phi) + \frac{\tau_n}{3}a_h(U^{n+1}, \phi) - m_h(\dot{U}_+^n, \phi) + \frac{\tau_n^2}{6}a_h(\dot{U}_+^n, \phi) = \frac{2}{\tau_n}m_h(U^n, \phi) \\ \quad - \frac{2\tau_n}{3}a_h(U^n, \phi) + m_h(\dot{U}_-^n, \phi) + \left(\int_{I_n} f_h(t) dt, \phi\right) \quad \forall \phi \in W_h, 0 \leq n \leq N-1, \\ \frac{1}{\tau_n}m_h(U^{n+1}, \eta) + \frac{\tau_n}{4}a_h(U^{n+1}, \eta) - m_h(\dot{U}_+^n, \eta) + \frac{\tau_n^2}{12}a_h(\dot{U}_+^n, \eta) = \frac{1}{\tau_n}m_h(U^n, \eta) \\ \quad - \frac{\tau_n}{4}a_h(U^n, \eta) + \left(\frac{1}{\tau_n} \int_{I_n} (t-t_n)f_h(t) dt, \eta\right) \quad \forall \eta \in W_h, 0 \leq n \leq N-1, \\ U^0 = \Psi_{0,h}, \quad \dot{U}_-^0 = \Psi_{1,h}. \end{cases} \tag{3.5}$$

It is easy to see from the method (3.5) that along the time direction, the numerical solution can be computed one interval after another.

Lemma 3.1. *In view of similar arguments as given in [21], if U is the solution of (3.2) with $f_h = 0$, and the initial function U^0 and \dot{U}_-^0 arbitrary given, then there hold*

$$\max_{0 \leq t \leq T} (\|\dot{U}(t_-)\|_{0,h}^2 + |U(t)|_{1,h}^2) + \sum_{n=0}^{N-1} \|\dot{U}_+^n\|_{0,h}^2 \lesssim \|U^0\|_{1,h}^2 + \|\dot{U}_-^0\|_{0,h}^2 \tag{3.6}$$

and

$$\|\dot{U}\|_{\infty,0,h} \lesssim (|U^0|_{1,h} + \|\dot{U}_-^0\|_{0,h}). \tag{3.7}$$

The first inequality (3.6) ensures the unique solvability of (3.2).

4. Some fundamental results. We now present some preliminary results useful in the sequel.

4.1. Error estimates for static problems. Consider the variational formulation of the static problem of (2.1) and its virtual element discretized problem, described as follows.

$$\begin{cases} \text{Find } u \in V \text{ such that} \\ a(u, v) = (f, v) \quad \forall v \in V. \end{cases} \tag{4.1}$$

$$\begin{cases} \text{Find } u_h \in W_h \text{ such that} \\ a_h(u_h, v_h) = (f_h, v_h) \quad \forall v_h \in W_h. \end{cases} \tag{4.2}$$

Following the ideas for deriving error estimates of the VEM in [2] and exploiting some estimates in [16], we can easily obtain the following lemma.

Lemma 4.1. *Let u be the solution of (4.1), and let $u_h \in W_h$ be the solution of (4.2), with W_h defined in (2.8), a_h defined in (2.9), and f_h defined in (2.12). Assume further that Ω is convex, the right-hand side $f \in H^k(\Omega)$, and the exact solution u of (4.1) belongs to $H^{k+1}(\Omega)$. Then there holds*

$$\|u - u_h\|_{0,\Omega} + h|u - u_h|_{1,\Omega} \lesssim h^{k+1}|u|_{k+1,\Omega}. \tag{4.3}$$

4.2. The backward homogeneous problem. Consider the dual problem of (2.1) with $f = 0$, described as follows.

$$\begin{cases} \ddot{G} - \Delta G = 0 & \text{in } \Omega \times I, \\ G = 0 & \text{on } \partial\Omega \times I, \\ G(\cdot, T) = \Phi_0, \dot{G}(\cdot, T) = \Phi_1 & \text{in } \Omega. \end{cases} \quad (4.4)$$

By introducing a time transformation $\tilde{t} = T - t$, we can rewrite (4.4) as the same form for (2.1). We then use the C^0P_2 time stepping VEM (3.2) to solve this problem, and the numerical scheme is equivalent to finding $g \in S^{h\tau}$ such that

$$\begin{cases} \int_{I_n} (m_h(\dot{v}, \ddot{g}) + a_h(\dot{v}, g)) dt + m_h(\dot{v}_{-}^{n+1}, [\dot{g}]_{n+1}) = 0 \quad \forall v \in S_n^{h\tau}, 0 \leq n \leq N-1, \\ g^N = \Phi_{0,h}, \dot{g}_+^N = \Phi_{1,h}, \end{cases} \quad (4.5)$$

where $\Phi_{0,h}$ and $\Phi_{1,h}$ are arbitrary functions in W_h . Summing over n from 0 to $N-1$ yields

$$\sum_{n=0}^{N-1} \int_{I_n} (m_h(\dot{v}, \ddot{g}) + a_h(\dot{v}, g)) dt + \sum_{n=0}^{N-1} m_h(\dot{v}_{-}^{n+1}, [\dot{g}]_{n+1}) = 0 \quad \forall v \in S^{h\tau}. \quad (4.6)$$

According to the Lemma 3.1, the function $g \in S^{h\tau}$ given by (4.5) satisfies

$$\|\dot{g}\|_{\infty,0,h} \lesssim (\|\Phi_{0,h}\|_{1,h} + \|\Phi_{1,h}\|_{0,h}). \quad (4.7)$$

4.3. The time-direction interpolation operators Q_τ . Along the time direction, introduce the local quadratic interpolation operators $Q_n : C^1(\bar{I}_n) \rightarrow \mathbb{P}_2(I_n)$ by

$$\begin{cases} (Q_n v)^n = v^n, \\ (Q_n v)^{n+1} = v^{n+1}, \\ (Q_n v)_{t_-}^{n+1} = \dot{v}^{n+1}, \end{cases} \quad (4.8)$$

for $n = 0, 1, \dots, N-1$. It is easy to check that

$$\int_{I_n} (Q_n v)_t dt = \int_{I_n} \dot{v} dt. \quad (4.9)$$

With these operators, we then denote the global interpolation operator $Q_\tau : C^1(\bar{I}) \rightarrow \prod_{n=0}^{N-1} (\mathbb{P}_2(I_n))$ by

$$Q_\tau v = Q_n v \text{ on } I_n, 0 \leq n \leq N-1, \forall v \in C^1(\bar{I}).$$

The following lemma presents an error bound for the interpolation operator Q_τ (cf. [15]).

Lemma 4.2. *For any function $v \in C^1(\bar{I})$ with $v_{ttt} \in L^p(I)$, there holds*

$$\|v - Q_\tau v\|_{L^p(I)} \lesssim \tau^3 \|v_{ttt}\|_{L^p(I)}, \quad (4.10)$$

where $1 \leq p \leq \infty$ and $v_{ttt} := \partial^3 v / \partial t^3$.

5. Error estimates for the C^0P_2 time-stepping VEM. In this section, we will develop error analysis for the C^0P_2 time stepping VEM (3.2). Throughout this section, we assume that the exact solution u of (2.1) satisfies the following regularity conditions

$$u \in L^\infty(0, T; H^{k+1}(\Omega) \cap H_0^1(\Omega)), \quad u_t \in L^\infty(0, T; H^{k+1}(\Omega)), \quad (5.1)$$

and

$$u_{tt} \in L^1(0, T; H^{k+1}(\Omega)), \quad u_{ttt} \in L^1(0, T; H^2(\Omega)). \quad (5.2)$$

Write

$$e := u - U = e_1 - e_2, \quad (5.3)$$

where $e_1 := u - Q_\tau(\mathcal{P}^\nabla u)$ and $e_2 := U - Q_\tau(\mathcal{P}^\nabla u)$. For clarity, we divide our error analysis into three steps.

Step 1. The estimate for e_1 . By (4.8) and (2.17),

$$\begin{aligned} |e_1(t_N)|_{1,\Omega} &= |u(t_N) - (Q_\tau(\mathcal{P}^\nabla u))(t_N)|_{1,\Omega} = |u(t_N) - (\mathcal{P}^\nabla u)(t_N)|_{1,\Omega} \\ &\lesssim h^k |u(t_N)|_{k+1,\Omega} \lesssim h^k |u|_{\infty,k+1}. \end{aligned} \quad (5.4)$$

Observing that the time derivative is commutative with the modified H^1 projection \mathcal{P}^∇ , we have by (4.8) and (2.18) that

$$\begin{aligned} \|(\dot{e}_1)_-^N\|_{0,\Omega} &= \|((u - \mathcal{P}^\nabla u)_t)_-^{t_N}\|_{0,\Omega} = \|((I - \mathcal{P}^\nabla)u_t)_-^{t_N}\|_{0,\Omega} \\ &\lesssim h^{k+1} |u_t(t_N)|_{k+1,\Omega} \lesssim h^{k+1} |u_t|_{\infty,k+1}. \end{aligned} \quad (5.5)$$

Step 2. The estimate for e_2 . Using (2.1) combined with an integration by parts, we find

$$\int_{I_n} ((\ddot{u}, \dot{v})_{L^2(\Omega)} + a(u, \dot{v})) dt = \int_{I_n} (f, \dot{v}) dt \quad \forall v \in S_n^{h\tau}, \quad 0 \leq n \leq N-1. \quad (5.6)$$

Then by the definition of \mathcal{P}^∇ (resp. \mathcal{P}^0) (2.13) (resp. (2.16)), (5.6) is equivalent to

$$\int_{I_n} (m_h(\mathcal{P}^0 \ddot{u}, \dot{v}) + a_h(\mathcal{P}^\nabla u, \dot{v})) dt = \int_{I_n} (f, \dot{v}) dt \quad \forall v \in S_n^{h\tau}, \quad 0 \leq n \leq N-1. \quad (5.7)$$

Subtracting the first equation of (3.2) from (5.7), and using the fact that $[\dot{u}]_n = 0$ for $0 \leq n \leq N-1$, we obtain

$$\int_{I_n} (m_h(\mathcal{P}^0 \ddot{u} - \ddot{U}, \dot{v}) + a_h(\mathcal{P}^\nabla u - U, \dot{v})) dt + m_h([\dot{e}]_n, \dot{v}_+^n) = \int_{I_n} (f - f_h, \dot{v}) dt \quad \forall v \in S_n^{h\tau}.$$

Furthermore, we write the above equation associated with the initial conditions as follows.

$$\begin{cases} \int_{I_n} (m_h(\ddot{e}, \dot{v}) + a_h(e, \dot{v})) dt + m_h([\dot{e}]_n, \dot{v}_+^n) = \int_{I_n} E_h(u, \dot{v}) dt \quad \forall v \in S_n^{h\tau}, \\ e^0 = (I - \mathcal{P}^\nabla)\Psi_0, \quad \dot{e}_-^0 = (I - \mathcal{P}^\nabla)\Psi_1, \end{cases} \quad (5.8)$$

where

$$E_h(u, \dot{v}) := m_h((I - \mathcal{P}^0)\ddot{u}, \dot{v}) + a_h((I - \mathcal{P}^\nabla)u, \dot{v}) + (f - f_h, \dot{v}).$$

Inserting (5.3) into (5.8) and summing these equations over n from 0 to $N - 1$, we obtain the following identity:

$$\begin{aligned} & \sum_{n=0}^{N-1} \left(\int_{I_n} (m_h(\ddot{e}_2, \dot{v}) + a_h(e_2, \dot{v})) dt + m_h([\dot{e}_2]_n, \dot{v}_+^n) \right) \\ &= \sum_{n=0}^{N-1} \left(\int_{I_n} (m_h(\ddot{e}_1, \dot{v}) + a_h(e_1, \dot{v}) - E_h(u, \dot{v})) dt + m_h([\dot{e}_1]_n, \dot{v}_+^n) \right). \end{aligned} \quad (5.9)$$

We first simplify the LHS of (5.9). We have by integration by parts and a direct manipulation that

$$\begin{aligned} \text{LHS} &= \sum_{n=0}^{N-1} \left(\int_{I_n} (m_h(\ddot{e}_2, \dot{v}) + a_h(e_2, \dot{v})) dt + m_h([\dot{e}_2]_n, \dot{v}_+^n) \right) \\ &= \sum_{n=0}^{N-1} \left(m_h((\dot{e}_2)_-^{n+1}, \dot{v}_-^{n+1}) - m_h((\dot{e}_2)_-, \dot{v}_+^n) + a_h((e_2)^{n+1}, v^{n+1}) \right. \\ &\quad \left. - a_h((e_2)^n, v^n) - \int_{I_n} (m_h(\dot{e}_2, \ddot{v}) + a_h(\dot{e}_2, v)) dt \right) \\ &= - \sum_{n=0}^{N-1} \left(\int_{I_n} (m_h(\dot{e}_2, \ddot{v}) + a_h(\dot{e}_2, v)) dt + m_h((\dot{e}_2)_-^{n+1}, [\dot{v}]_{n+1}) \right) \\ &\quad + m_h((\dot{e}_2)_-^N, \dot{v}_+^N) - m_h((\dot{e}_2)_-, \dot{v}_+^0) + a_h((e_2)^N, v^N) - a_h((e_2)^0, v^0). \end{aligned} \quad (5.10)$$

The definition of Q_τ and (2.14) implies that

$$(\dot{e}_2)_-^0 = \dot{U}_-^0 - (\mathcal{P}^\nabla u)_t(0) = \dot{U}_-^0 - \mathcal{P}^\nabla u_t(0) = \Psi_{1,h} - \mathcal{P}^\nabla \Psi_1 = 0,$$

and

$$(e_2)^0 = U^0 - (\mathcal{P}^\nabla u)(0) = U^0 - \mathcal{P}^\nabla(u(0)) = \Psi_{0,h} - \mathcal{P}^\nabla \Psi_0 = 0.$$

Then (5.10) can be reformulated as

$$\begin{aligned} \text{LHS} &= \sum_{n=0}^{N-1} \left(\int_{I_n} (m_h(\ddot{e}_2, \dot{v}) + a_h(e_2, \dot{v})) dt + m_h([\dot{e}_2]_n, \dot{v}_+^n) \right) \\ &= - \sum_{n=0}^{N-1} \left(\int_{I_n} (m_h(\dot{e}_2, \ddot{v}) + a_h(\dot{e}_2, v)) dt + m_h((\dot{e}_2)_-^{n+1}, [\dot{v}]_{n+1}) \right) \\ &\quad + m_h((\dot{e}_2)_-^N, \dot{v}_+^N) + a_h((e_2)^N, v^N). \end{aligned} \quad (5.11)$$

Now, in order to simplify the expression, we choose v as g , where $g \in S^{h\tau}$ is the solution of (4.5). Then by using (4.6) we know the LHS of (5.9) satisfies

$$\begin{aligned} \text{LHS} &= \sum_{n=0}^{N-1} \left(\int_{I_n} (m_h(\ddot{e}_2, \dot{g}) + a_h(e_2, \dot{g})) dt + m_h([\dot{e}_2]_n, \dot{g}_+^n) \right) \\ &= m_h((\dot{e}_2)_-^N, \dot{g}_+^N) + a_h((e_2)^N, g^N). \end{aligned} \quad (5.12)$$

Next, we try to simplify the RHS of (5.9):

$$\begin{aligned} \text{RHS} &= \sum_{n=0}^{N-1} \left(\int_{I_n} (m_h(\ddot{e}_1, \dot{g}) + a_h(e_1, \dot{g}) - E_h(u, \dot{g})) dt + m_h([\dot{e}_1]_n, \dot{g}_+^n) \right) \\ &= \sum_{n=0}^{N-1} \left(\int_{I_n} (a_h((I - Q_\tau)(\mathcal{P}^\nabla u), \dot{g}) + (f - f_h, \dot{g})) dt \right. \\ &\quad \left. + \int_{I_n} m_h((\mathcal{P}^0 u - Q_\tau(\mathcal{P}^\nabla u))_{tt}, \dot{g}) dt + m_h([(u - Q_\tau(\mathcal{P}^\nabla u))_t]_n, \dot{g}_+^n) \right). \end{aligned} \quad (5.13)$$

Since $\mathcal{P}^0 u \in C^1(0, T; W_h)$ and $\mathcal{P}^\nabla u \in C^1(0, T; W_h)$, we have by (4.8) and (4.9) that

$$\begin{aligned} \int_{I_n} ((I - Q_\tau)(\mathcal{P}^\nabla u))_t dt &= 0, \quad [(\mathcal{P}^0 u - \mathcal{P}^\nabla u)_t]_n = 0, \\ ((I - Q_\tau)(\mathcal{P}^\nabla u))_{t-}^n &= 0, \quad ((I - Q_\tau)(\mathcal{P}^\nabla u))_{t-}^{n+1} = 0. \end{aligned}$$

Then using integration by parts and observing the fact \ddot{g} is piecewise constant in the time direction, we see that

$$\begin{aligned} &\int_{I_n} m_h((\mathcal{P}^0 u - Q_\tau(\mathcal{P}^\nabla u))_{tt}, \dot{g}) dt + m_h([(u - Q_\tau(\mathcal{P}^\nabla u))_t]_n, \dot{g}_+^n) \\ &= - \int_{I_n} m_h((\mathcal{P}^0 u - \mathcal{P}^\nabla u)_t, \ddot{g}) dt + m_h((\mathcal{P}^0 u - \mathcal{P}^\nabla u)_{t-}^{n+1}, \dot{g}_-^{n+1}) \\ &\quad - m_h((\mathcal{P}^0 u - \mathcal{P}^\nabla u)_{t-}^n, \dot{g}_+^n) - m_h\left(\int_{I_n} ((I - Q_\tau)(\mathcal{P}^\nabla u))_t dt, \ddot{g}\right) \\ &= -m_h((\mathcal{P}^0 u - \mathcal{P}^\nabla u)_t, \dot{g})|_{t_n}^{t_{n+1}} + \int_{I_n} m_h((\mathcal{P}^0 u - \mathcal{P}^\nabla u)_{tt}, \dot{g}) dt \\ &\quad + m_h((\mathcal{P}^0 u - \mathcal{P}^\nabla u)_{t-}^{n+1}, \dot{g}_-^{n+1}) - m_h((\mathcal{P}^0 u - \mathcal{P}^\nabla u)_{t-}^n, \dot{g}_+^n) \\ &= \int_{I_n} m_h((\mathcal{P}^0 u - \mathcal{P}^\nabla u)_{tt}, \dot{g}) dt. \end{aligned} \quad (5.14)$$

Therefore, in terms of (5.13) and (5.14), we can rewrite the RHS of (5.9) as

$$\begin{aligned} \text{RHS} &= \sum_{n=0}^{N-1} \left(\int_{I_n} (m_h(\ddot{e}_1, \dot{g}) + a_h(e_1, \dot{g}) - E_h(u, \dot{g})) dt + m_h([\dot{e}_1]_n, \dot{g}_+^n) \right) \\ &= \sum_{n=0}^{N-1} \left(\int_{I_n} \left(m_h((\mathcal{P}^0 u - \mathcal{P}^\nabla u)_{tt}, \dot{g}) + a_h((I - Q_\tau)(\mathcal{P}^\nabla u), \dot{g}) \right. \right. \\ &\quad \left. \left. + (f - f_h, \dot{g}) \right) dt \right). \end{aligned} \quad (5.15)$$

Hence, the combination of (5.9), (5.12) and (5.15) together implies

$$\begin{aligned} &m_h((\dot{e}_2)_-, \dot{g}_+^N) + a_h((e_2)^N, g^N) \\ &= \sum_{n=0}^{N-1} \int_{I_n} \left(m_h((\mathcal{P}^0 u - \mathcal{P}^\nabla u)_{tt}, \dot{g}) + a_h((I - Q_\tau)(\mathcal{P}^\nabla u), \dot{g}) \right. \\ &\quad \left. + (f - f_h, \dot{g}) \right) dt. \end{aligned} \quad (5.16)$$

Now, choosing g such that $g^N = (e_2)^N$ and $\dot{g}_+^N = 0$, from the stability of $a_h(\cdot, \cdot)$ and (5.16), we have

$$\begin{aligned} |(e_2)^N|_1^2 &\lesssim |(e_2)^N|_{1,h}^2 = a_h((e_2)^N, (e_2)^N) \\ &= \sum_{n=0}^{N-1} \int_{I_n} \left(m_h((\mathcal{P}^0 u - \mathcal{P}^\nabla u)_{tt}, \dot{g}) + a_h((I - Q_\tau)(\mathcal{P}^\nabla u), \dot{g}) + (f - f_h, \dot{g}) \right) dt \\ &= \text{I} + \text{II} + \text{III}, \end{aligned} \quad (5.17)$$

where

$$\begin{aligned} \text{I} &:= \sum_{n=0}^{N-1} \int_{I_n} m_h((\mathcal{P}^0 u - \mathcal{P}^\nabla u)_{tt}, \dot{g}) dt, \quad \text{II} := \sum_{n=0}^{N-1} \int_{I_n} a_h((I - Q_\tau)(\mathcal{P}^\nabla u), \dot{g}) dt, \\ \text{III} &:= \sum_{n=0}^{N-1} \int_{I_n} (f - f_h, \dot{g}) dt. \end{aligned}$$

Let us study the first term in the sum (5.17). By using the Cauchy-Schwarz inequality, the triangle inequality, (4.7), (2.18), (2.19) and the consistency property of the approximated H^1 semi-norm and L^2 norm, we have

$$\begin{aligned} |\text{I}| &\lesssim \sum_{n=0}^{N-1} \int_{I_n} \|(\mathcal{P}^0 u - \mathcal{P}^\nabla u)_{tt}\|_{0,h} \|\dot{g}(t)\|_{0,h} dt \lesssim \sum_{n=0}^{N-1} \int_{I_n} \|(\mathcal{P}^0 u - \mathcal{P}^\nabla u)_{tt}\|_{0,h} dt \|\dot{g}\|_{\infty,0,h} \\ &\lesssim \sum_{n=0}^{N-1} \int_{I_n} \|(\mathcal{P}^0 u - \mathcal{P}^\nabla u)_{tt}\|_{0,h} dt |(e_2)^N|_{1,h} \lesssim \sum_{n=0}^{N-1} \int_{I_n} \|(\mathcal{P}^0 u - \mathcal{P}^\nabla u)_{tt}\|_0 dt |(e_2)^N|_1 \\ &\lesssim \sum_{n=0}^{N-1} \int_{I_n} (\|(u - \mathcal{P}^\nabla u)_{tt}\|_0 + \|(u - \mathcal{P}^0 u)_{tt}\|_0) dt |(e_2)^N|_1 \\ &\lesssim h^{k+1} \|u_{tt}\|_{L^1(0,T; H^{k+1}(\Omega))} |(e_2)^N|_1. \end{aligned} \quad (5.18)$$

For the second term, since the time derivative is commutative with \mathcal{P}^∇ (resp. \mathcal{P}^0), we have by integration by parts that

$$\begin{aligned} \text{II} &= \sum_{n=0}^{N-1} \int_{I_n} a_h(\mathcal{P}^\nabla((I - Q_\tau)u), \dot{g}) dt = \sum_{n=0}^{N-1} \int_{I_n} a((I - Q_\tau)u, \dot{g}) dt \\ &= \sum_{n=0}^{N-1} \int_{I_n} (-(I - Q_\tau)(\Delta u), \dot{g})_{L^2(\Omega)} dt = \sum_{n=0}^{N-1} \int_{I_n} m_h(\mathcal{P}^0(-(I - Q_\tau)(\Delta u)), \dot{g}) dt. \\ &= \sum_{n=0}^{N-1} \int_{I_n} m_h((I - Q_\tau)(\mathcal{P}^0(-\Delta u)), \dot{g}) dt. \end{aligned}$$

Hence, according to the Cauchy-Schwarz inequality, the coercivity of $m_h(\cdot, \cdot)$, (4.7) and (4.10),

$$\begin{aligned} |\text{III}| &\lesssim \sum_{n=0}^{N-1} \int_{I_n} \|(I - Q_\tau)(\mathcal{P}^0(-\Delta u))\|_{0,h} dt \|\dot{g}\|_{\infty,0,h} \\ &\lesssim \sum_{n=0}^{N-1} \int_{I_n} \|(I - Q_\tau)(-\Delta u)\|_0 dt |(e_2)^N|_1 \\ &\lesssim \tau^3 \|u_{ttt}\|_{L^1(0,T; H^2(\Omega))} |(e_2)^N|_1. \end{aligned} \quad (5.19)$$

For the last term, we find by the Cauchy-Schwarz inequality and (2.12) that

$$\begin{aligned}
 |\text{III}| &= \left| \sum_{n=0}^{N-1} \int_{I_n} \left(\sum_{E \in \mathcal{T}_n} \int_E (f(t) - \Pi_k^{0,E} f(t)) \dot{g} \, dx \right) dt \right| \\
 &\lesssim \sum_{n=0}^{N-1} \int_{I_n} h^{k+1} \|f(t)\|_{k+1} \|\dot{g}(t)\|_0 \, dt \lesssim h^{k+1} \sum_{n=0}^{N-1} \int_{I_n} \|f(t)\|_{k+1} \, dt \|\dot{g}(t)\|_{\infty,0} \\
 &\lesssim h^{k+1} \sum_{n=0}^{N-1} \int_{I_n} \|f(t)\|_{k+1} \, dt |(e_2)^N|_1 \\
 &\lesssim h^{k+1} \|f\|_{L^1(0,T; H^{k+1}(\Omega))} |(e_2)^N|_1.
 \end{aligned} \tag{5.20}$$

Finally, inserting the estimates (5.18), (5.19) and (5.20) into (5.17), we arrive at

$$\begin{aligned}
 |(e_2)^N|_1 &\lesssim \left(h^{k+1} \|u_{tt}\|_{L^1(0,T; H^{k+1}(\Omega))} + \tau^3 \|u_{ttt}\|_{L^1(0,T; H^2(\Omega))} \right. \\
 &\quad \left. + h^{k+1} \|f\|_{L^1(0,T; H^{k+1}(\Omega))} \right).
 \end{aligned} \tag{5.21}$$

If we take

$$g^N = 0, \quad \dot{g}_+^N = (\dot{e}_2)_-^N$$

in (5.16) and then use the similar arguments for deriving (5.21), we can obtain

$$\begin{aligned}
 \|(\dot{e}_2)_-^N\|_0 &\lesssim \left(h^{k+1} \|u_{tt}\|_{L^1(0,T; H^{k+1}(\Omega))} + \tau^3 \|u_{ttt}\|_{L^1(0,T; H^2(\Omega))} \right. \\
 &\quad \left. + h^{k+1} \|f\|_{L^1(0,T; H^{k+1}(\Omega))} \right).
 \end{aligned} \tag{5.22}$$

Step 3. The estimate for e . Combining (5.4), (5.5), (5.21) and (5.22) obtained in Steps 1 and 2 and using the triangle inequality

$$\|e\| \leq \|e_1\| + \|e_2\|,$$

where $\|\cdot\|$ stands for the norm $|\cdot|_{1,\Omega}$ or $\|\cdot\|_{0,\Omega}$, we can readily derive the desired error estimates for the numerical method (3.2), described as the following theorem.

Theorem 5.1. *Let u and U be the solutions of (2.1) and (3.2), respectively. Assume u satisfies the regularity conditions (5.1) and (5.2). Then for $n = 1, 2, \dots, N$, there hold*

$$\begin{aligned}
 |u(t_n) - U^n|_{1,\Omega} &\lesssim h^k |u|_{\infty,k+1} + h^{k+1} \left(\|u_{tt}\|_{L^1(0,T; H^{k+1}(\Omega))} + \|f\|_{L^1(0,T; H^{k+1}(\Omega))} \right) \\
 &\quad + \tau^3 \|u_{ttt}\|_{L^1(0,T; H^2(\Omega))}
 \end{aligned} \tag{5.23}$$

and

$$\begin{aligned}
 \|\dot{u}(t_n) - \dot{U}_-^n\|_{0,\Omega} &\lesssim h^{k+1} \left(|u_t|_{\infty,k+1} + \|u_{tt}\|_{L^1(0,T; H^{k+1}(\Omega))} + \|f\|_{L^1(0,T; H^{k+1}(\Omega))} \right) \\
 &\quad + \tau^3 \|u_{ttt}\|_{L^1(0,T; H^2(\Omega))}.
 \end{aligned} \tag{5.24}$$

Corollary 1. *Under the conditions in Theorem 5.1, for $n = 1, 2, \dots, N$, there holds*

$$\begin{aligned}
 \|u(t_n) - U^n\|_{0,\Omega} &\lesssim h^{k+1} \left(|u|_{\infty,k+1} + \|u_{tt}\|_{L^1(0,T; H^{k+1}(\Omega))} + \|f\|_{L^1(0,T; H^{k+1}(\Omega))} \right) \\
 &\quad + \tau^3 \|u_{ttt}\|_{L^1(0,T; H^2(\Omega))}.
 \end{aligned} \tag{5.25}$$

Remark 3. For our method (3.2), if choosing $k = 2$ and adopting uniformly temporal discretization, we have from the above estimate that $\|u(t_n) - U^n\|_{0,\Omega} = O(h^3 + \tau^3)$.

6. Numerical results. In this section, we present several numerical experiments on the operating platform (Matlab R2016a on MacOS10.12.6) to show the performance of the C^0P_2 time-stepping VEM (3.2). The codes are designed based on the references [5, 25] and polygonal Voroni meshes \mathcal{V}_h are produced using the software Polymesher introduced in [26].

Theoretically, the error generated by a fully discrete scheme has two components: the error due to the spatial discretization depending on h , and the error created by the time integrator depending on τ . In particular, let $\{U^n\}_{n=0}^N$ be the function sequence generated by the method (3.2), where $U^n = U(\cdot, t_n)$ for $n = 0, 1, \dots, N$.

Define

$$\begin{aligned} E_{H^1} &= \max_{1 \leq n \leq N} |u(t_n) - U^n|_{1,h} \approx \max_{1 \leq n \leq N} \left((\mathbf{u}(t_n) - \mathbf{U}^n)^T \mathbf{K} (\mathbf{u}(t_n) - \mathbf{U}^n) \right)^{1/2}, \\ Et_{L^2} &= \max_{1 \leq n \leq N} \|u_t(t_n) - \dot{U}_-^n\|_{0,h} \approx \max_{1 \leq n \leq N} \left((\mathbf{u}_t(t_n) - \dot{\mathbf{U}}_-^n)^T \mathbf{M} (\mathbf{u}_t(t_n) - \dot{\mathbf{U}}_-^n) \right)^{1/2}, \\ E_{L^2} &= \max_{1 \leq n \leq N} \|u(t_n) - U^n\|_{0,h} \approx \max_{1 \leq n \leq N} \left((\mathbf{u}(t_n) - \mathbf{U}^n)^T \mathbf{M} (\mathbf{u}(t_n) - \mathbf{U}^n) \right)^{1/2}, \end{aligned}$$

where \mathbf{K} and \mathbf{M} are the related stiffness and mass matrices, respectively.

And introduce the experimental order of convergence:

$$EOC := \frac{\log(Err/Err')}{\log(h/h')} \quad \text{or} \quad EOC := \frac{\log(Err/Err')}{\log(\tau/\tau')},$$

where Err and Err' are the errors on two consecutive grids with space mesh-size h and h' or time division-size τ and τ' , respectively.

We use the approximated H^1 semi-norm and L^2 norm to study the orders of the error E_{H^1} , Et_{L^2} and E_{L^2} with respect to h and τ , respectively.

Example 6.1. Consider the problem (2.1) defined on the unit square $\Omega = (0, 1)^2$ and choose the time interval $I = (0, 1)$. We take the load term f , the initial data Ψ_0 and Ψ_1 to be in accordance with the exact solution

$$u(x_1, x_2, t) = \sin(\pi x_1) \sin(\pi x_2) \sin(t^2).$$

We will choose the orders of the VEM approximation as $k = 1$ and $k = 2$. For simplicity, we adopt the C^0P_2 element with the uniform division in the time discretization.

Case 1. $k = 1$

Firstly, in order to observe the convergence order of error E_{H^1} , Et_{L^2} in space direction, we fix time-division size $\tau = 1/40$ and let h vary from $1/5$ to $1/80$. The numerical results shown in Table 1 and Figure 2 in the log scale indicate that E_{H^1} is 1st-order and Et_{L^2} is 2nd-order in space direction.

TABLE 1. E_{H^1}, Et_{L^2} vs h : fixed $\tau = 1/40$ and h varies from $1/5$ to $1/80$ for $k = 1$.

h	1/5	1/10	1/20	1/40	1/80
E_{H^1}	4.838e-2	2.438e-2	1.266e-2	5.582e-3	2.968e-3
Et_{L^2}	1.866e-2	4.734e-3	1.191e-3	2.837e-4	7.381e-5

Then we consider the order of error E_{H^1} , Et_{L^2} with respect to τ . In this case, we take $h = \tau^3$ and $h^2 = \tau^3$ so that we can decrease the heavy computational cost

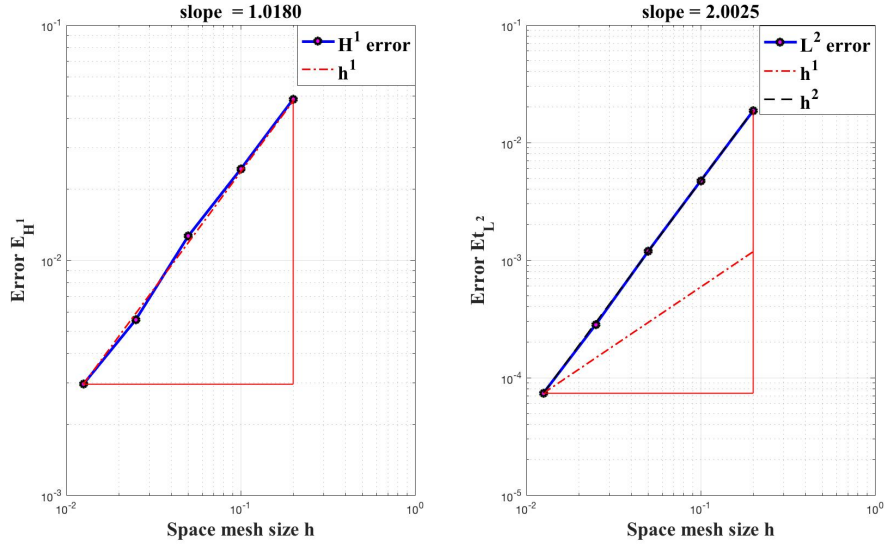


FIGURE 2. The orders of errors E_{H^1} and Et_{L^2} in space direction for $k = 1$.

but still illustrate the need results. For E_{H^1} , we choose $\tau = 1/2, 1/3, 1/4, 1/5, 1/6$ with the space mesh size $h = \tau^3$ in scheme (3.2). Similarly, for Et_{L^2} , we set $\tau = 1/4, 1/6, 1/8, 1/10, 1/12, 1/14, 1/16$ with the space mesh size $h^2 = \tau^3$. From Table 2 and 3, and Figure 3, we can see that both E_{H^1} and Et_{L^2} in our method proposed in (3.2) have 3-rd order accuracy in time direction.

TABLE 2. E_{H^1} vs τ : τ varies from 1/2 to 1/6 with $h = \tau^3$ for $k = 1$.

τ	1/2	1/3	1/4	1/5	1/6
E_{H^1}	5.435e-2	1.703e-2	7.083e-3	3.622e-3	2.073e-3

TABLE 3. Et_{L^2} vs τ : τ varies from 1/4 to 1/16 with $h^2 = \tau^3$ for $k = 1$.

τ	1/4	1/6	1/8	1/10	1/12	1/14	1/16
Et_{L^2}	9.738e-3	3.190e-3	1.350e-3	6.932e-4	3.955e-4	2.501e-4	1.647e-4

Finally, we consider the error bound of the C^0P_2 time stepping VEM proposed in (3.2). We take $h = 1/2^{j+1}$, $j = 1, \dots, 6$ with $h = \tau$ to generate different meshes, and show the numerical results in Table 4 and Figure 6. From the 4th and 7th column of Table 4, we observe that the ratios between E_{H^1} (resp. Et_{L^2}) and $h + \tau^3$ (resp. $h^2 + \tau^3$) can be controlled a bounded quantity, which indicates that there exists some absolute positive constant C such that

$$E_{H^1} \leq C(h + \tau^3) \text{ and } Et_{L^2} \leq C(h^2 + \tau^3).$$

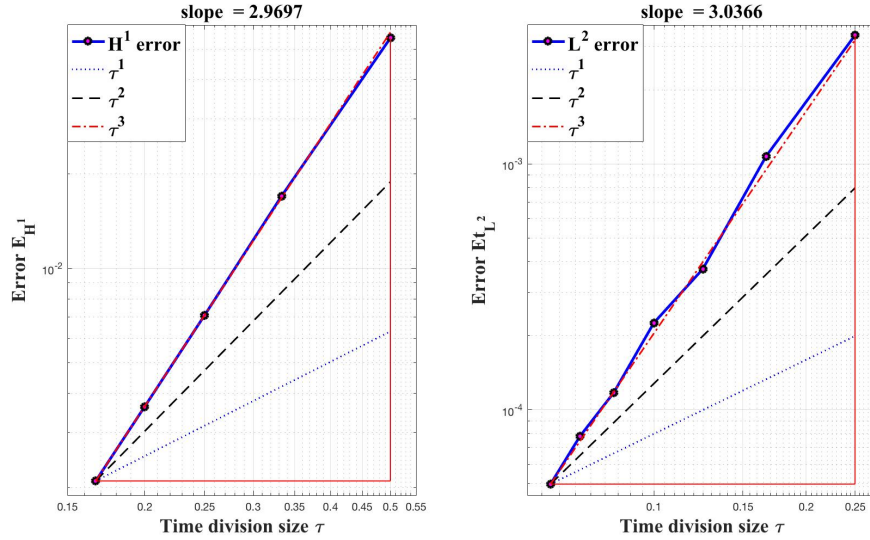


FIGURE 3. The orders of errors E_{H^1} and Et_{L^2} in time direction for $k = 1$.

TABLE 4. Error results with different meshes for $k = 1$.

$h = \tau$	#Dofs	E_{H^1}	$\frac{E_{H^1}}{h + \tau^3}$	$\frac{E_{H^1}}{\ u\ _{1,h}}$	Et_{L^2}	$\frac{Et_{L^2}}{h^2 + \tau^3}$	$\frac{Et_{L^2}}{\ u\ _{0,h}}$
1/4	34	6.731e-2	0.2534	3.770e-2	4.215e-2	0.5395	6.897e-2
1/8	130	2.823e-2	0.2227	1.528e-2	7.310e-3	0.4158	1.172e-2
1/16	510	1.328e-2	0.2116	7.121e-3	1.832e-3	0.4413	2.867e-3
1/32	2047	6.990e-3	0.2235	3.742e-3	4.507e-4	0.4476	7.031e-4
1/64	8160	3.464e-3	0.2216	1.853e-3	1.069e-4	0.4310	1.666e-4
1/128	32630	1.767e-3	0.2262	9.455e-4	2.666e-5	0.4333	4.154e-5

In addition, from the 5th and 8th column of Table 4 and Figure 6, we can see that the relative errors are also decreasing when mesh sizes are refined.

Case 2. $k = 2$

In this case, we perform the similar experiments as for $k = 1$. Firstly, in order to observe the convergence order of error E_{H^1} , Et_{L^2} in space direction, we fix time-division size $\tau = 1/80$ and let h vary from $1/5$ to $1/80$. The numerical results shown in Table 5 and Figure 4 in the log scale indicate that E_{H^1} is 2nd-order and Et_{L^2} is 3rd-order in space direction.

Then we consider the order of error E_{H^1} , Et_{L^2} with respect to τ . In this case, we take $h^2 = \tau^3$ and $h = \tau$ so that we can decrease the heavy computational cost but still illustrate the needed convergence orders. For E_{H^1} , we choose $\tau = 1/4, 1/6, 1/8, 1/10, 1/12, 1/14, 1/16$ with the space mesh size $h^2 = \tau^3$ in scheme

TABLE 5. E_{H^1}, Et_{L^2} vs h : fixed $\tau = 1/80$ and h varies from $1/5$ to $1/80$ for $k = 2$.

h	1/5	1/10	1/20	1/40	1/80
E_{H^1}	1.240e-2	1.994e-3	4.234e-4	9.892e-5	2.496e-5
Et_{L^2}	8.610e-3	3.312e-4	3.158e-5	3.585e-6	6.723e-7

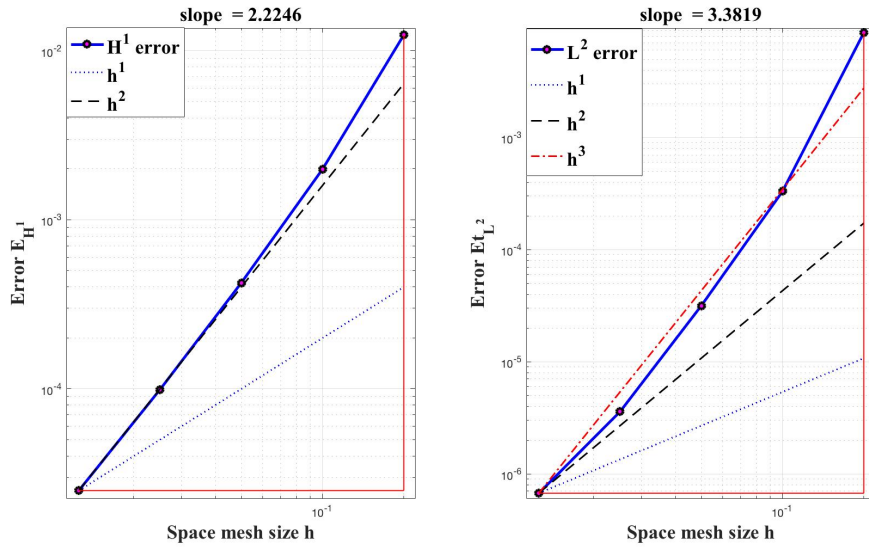


FIGURE 4. The orders of errors E_{H^1} and Et_{L^2} in space direction for $k = 2$.

(3.2). Similarly, for Et_{L^2} , we set $\tau = 1/2, 1/4, 1/8, 1/16, 1/32, 1/64, 1/128$ with the space mesh size $h = \tau$. From Table 6 and 7, and Figure 5, we can see that both E_{H^1} and Et_{L^2} in our method proposed in (3.2) have 3-rd order accuracy in time direction.

TABLE 6. E_{H^1} vs τ : τ varies from $1/4$ to $1/16$ with $h^2 = \tau^3$ for $k = 2$.

τ	1/4	1/6	1/8	1/10	1/12	1/14	1/16
E_{H^1}	7.333e-3	1.990e-3	8.194e-4	4.040e-4	2.322e-4	1.449e-4	9.702e-5

TABLE 7. Et_{L^2} vs τ : τ varies from $1/4$ to $1/128$ with $h = \tau$ for $k = 2$.

τ	1/4	1/8	1/16	1/32	1/64	1/128
Et_{L^2}	1.970e-2	1.021e-3	9.013e-5	1.056e-5	1.319e-6	1.631e-7

Finally, we consider the error bound of the C^0P_2 time stepping VEM proposed in (3.2). We take $h = 1/2^{j+1}$, $j = 1, \dots, 6$ with $h = \tau$ to generate different meshes, and show the numerical results in Table 8 and Figure 6. From the 4th and 7th

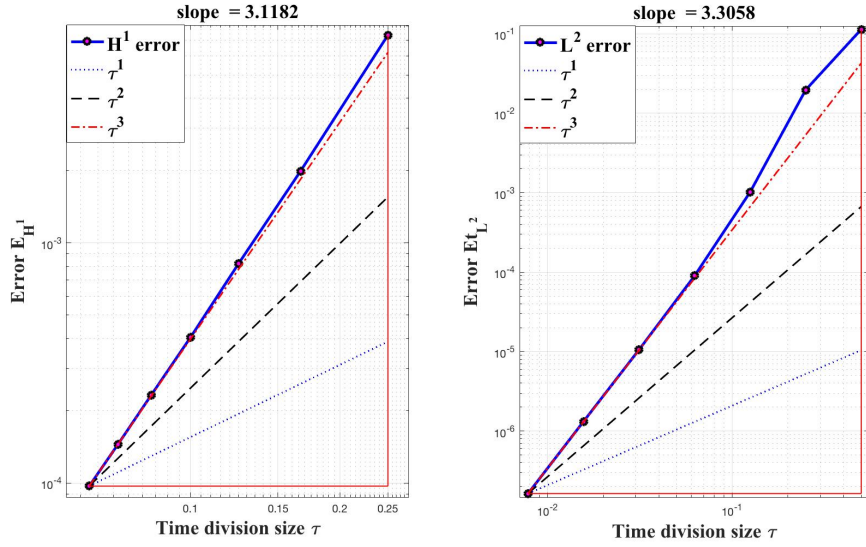


FIGURE 5. The orders of errors E_{H^1} and Et_{L^2} in time direction for $k = 2$.

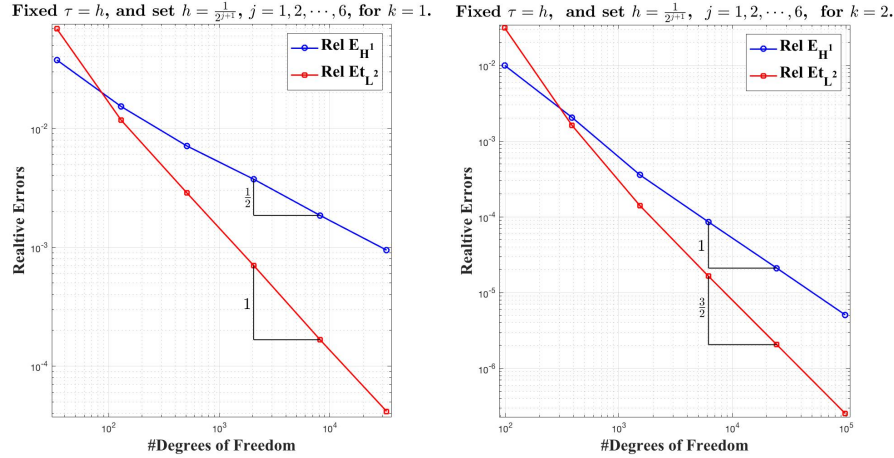


FIGURE 6. The orders of relative errors vs #Dofs for $k = 1$ and $k = 2$.

column of Table 8, we observe that the ratio between E_{H^1} (resp. Et_{L^2}) and $h^2 + \tau^3$ (resp. $h^3 + \tau^3$) can be controlled a bounded quantity, which indicates that there exists some absolute positive constant C such that

$$E_{H^1} \leq C(h^2 + \tau^3) \text{ and } Et_{L^2} \leq C(h^3 + \tau^3).$$

In addition, from the 5th and 8th column of Table 8, we can see that the relative errors are also decreasing when mesh sizes are refined.

TABLE 8. Error results with different meshes for $k = 2$.

$h = \tau$	#Dofs	E_{H^1}	$\frac{E_{H^1}}{h+\tau^3}$	$\frac{E_{H^1}}{\ u\ _{0,h}}$	Et_{L^2}	$\frac{Et_{L^2}}{h^2+\tau^3}$	$\frac{Et_{L^2}}{\ u\ _{0,h}}$
1/4	99	1.858e-2	0.2378	9.946e-3	1.970e-2	0.6303	3.105e-2
1/8	387	3.828e-3	0.2178	2.048e-3	1.027e-3	0.2613	1.609e-3
1/16	1531	6.684e-4	0.1610	3.576e-4	9.013e-5	0.1846	1.404e-4
1/32	6141	1.601e-4	0.1589	8.562e-5	1.056e-5	0.1730	1.646e-5
1/64	24511	3.932e-5	0.1586	2.104e-5	1.320e-6	0.1729	2.056e-6
1/128	98027	9.501e-6	0.1545	5.083e-6	1.631e-7	0.1711	2.542e-7

All the numerical results for $k = 1$ and $k = 2$ are in agreement with the theoretical results in Theorem 5.1.

Example 6.2. In this example, we make a numerical comparison between our method (3.2) and the Newmark trapezoidal VEM (see [27]). Assume the functions f , Ψ_0 and Ψ_1 in the problem (2.1) are given such that it has the following exact solution:

$$u(x_1, x_2, t) = e^{-t}(x_1^2 - x_1)(x_2^2 - x_2).$$

We use the Voronoi meshes for the solution domain $\Omega = (0, 1)^2$ and the uniform meshes for the time interval $I := (0, 1)$. The chosen orders of the VEM approximation are $k = 1$ and $k = 2$. The results of the approximated L^2 -norm error E_{L^2} are shown in Table 9.

TABLE 9. The comparison of E_{L^2} : method (3.2) vs the Newmark trapezoidal VEM.

$\tau = h$			C^0P_2 time-stepping VEM			Newmark trapezoidal VEM		
k	h	#Dofs	E_{L^2}	$\frac{E_{L^2}}{h^{k+1}+\tau^3}$	$\frac{E_{L^2}}{\ u\ _{0,h}}$	E_{L^2}	$\frac{E_{L^2}}{h^{k+1}+\tau^2}$	$\frac{E_{L^2}}{\ u\ _{0,h}}$
1	1/5	50	1.119e-3	2.331e-2	3.480e-2	1.167e-3	1.458e-2	3.629e-2
	1/10	202	2.754e-4	2.504e-2	8.354e-3	2.806e-4	1.403e-2	8.512e-3
	1/20	801	7.751e-5	2.953e-2	2.332e-3	7.786e-5	1.557e-2	2.343e-3
	1/40	3189	2.088e-5	3.259e-2	6.269e-4	2.099e-5	1.679e-2	6.301e-4
	1/80	12760	5.097e-6	3.222e-2	1.529e-4	5.115e-6	1.637e-2	1.535e-4
2	1/5	149	2.136e-4	1.335e-2	6.405e-3	2.267e-4	4.723e-3	6.798e-3
	1/10	603	2.074e-5	1.037e-2	6.222e-4	2.211e-5	2.010e-3	6.632e-4
	1/20	2401	2.916e-6	1.166e-2	8.747e-5	3.096e-6	1.179e-3	9.287e-5
	1/40	9577	3.605e-7	1.154e-2	1.081e-5	4.927e-7	7.691e-4	1.478e-5
	1/80	38319	4.535e-8	1.161e-2	1.360e-6	1.152e-7	7.285e-4	3.458e-6

From Table 9 we can observe that for both cases, the two methods have the expected order of convergence in h , that is, $O(h^{k+1})$. However, if we consider the error effect from temporal discretization together, we can find from the 4-th, 5-th, 7-th and 8-th columns of Table 9 that the error E_{L^2} is actually $O(h^{k+1} + \tau^3)$ for the C^0P_2 time-stepping VEM while $O(h^{k+1} + \tau^2)$ for the Newmark trapezoidal VEM. Therefore, our method performs better than the latter one in the time direction.

Acknowledgments. The authors would like to thank the referees for their valuable comments leading to an improvement of the early version of the paper.

REFERENCES

- [1] R. A. Adams, *Sobolev Spaces*, Pure and Applied Mathematics, Vol. 65. Academic Press, New York-London, 1975.
- [2] B. Ahmad, A. Alsaedi, F. Brezzi, L. D. Marini and A. Russo, [Equivalent projectors for virtual element methods](#), *Comput. Math. Appl.*, **66** (2013), 376–391.
- [3] L. Beirão da Veiga, F. Brezzi, A. Cangiani, G. Manzini, L. D. Marini and A. Russo, [Basic principles of virtual element methods](#), *Math. Models Methods Appl. Sci.*, **23** (2013), 199–214.
- [4] L. Beirão da Veiga, F. Brezzi and L. D. Marini, [Virtual elements for linear elasticity problems](#), *SIAM J. Numer. Anal.*, **51** (2013), 794–812.
- [5] L. Beirão da Veiga, F. Brezzi, L. D. Marini and A. Russo, [The hitchhiker’s guide to the virtual element method](#), *Math. Models Methods Appl. Sci.*, **24** (2014), 1541–1573.
- [6] L. Beirão da Veiga, F. Brezzi, L. D. Marini and A. Russo, [Serendipity nodal VEM spaces](#), *Comput. & Fluids*, **141** (2016), 2–12.
- [7] L. Beirão da Veiga, F. Brezzi, L. D. Marini and A. Russo, [Virtual element method for general second-order elliptic problems on polygonal meshes](#), *Math. Models Methods Appl. Sci.*, **26** (2016), 729–750.
- [8] L. Beirão da Veiga, F. Dassi and A. Russo, [High-order virtual element method on polyhedral meshes](#), *Comput. Math. Appl.*, **74** (2017), 1110–1122.
- [9] L. Beirão da Veiga, C. Lovadina and D. Mora, [A virtual element method for elastic and inelastic problems on polytope meshes](#), *Comput. Methods Appl. Mech. Engrg.*, **295** (2015), 327–346.
- [10] S. C. Brenner and L. R. Scott, *The Mathematical Theory of Finite Element Methods*, Third edition, Texts in Applied Mathematics, 15. Springer, New York, 2008.
- [11] F. Brezzi, The great beauty of VEMs, *Proceedings of the International Congress of Mathematicians - Seoul 2014*, Kyung Moon Sa, Seoul, **1** (2014), 217–234.
- [12] F. Brezzi, A. Buffa and K. Lipnikov, [Mimetic finite differences for elliptic problems](#), *M2AN Math. Model. Numer. Anal.*, **43** (2009), 277–295.
- [13] F. Brezzi and L. D. Marini, [Virtual element methods for plate bending problems](#), *Comput. Methods Appl. Mech. Engrg.*, **253** (2013), 455–462.
- [14] A. Cangiani, G. Manzini and O. J. Sutton, [Conforming and nonconforming virtual element methods for elliptic problems](#), *IMA J. Numer. Anal.*, **37** (2017), 1317–1354.
- [15] C. Chen, *Structure Theory of Superconvergence of Finite Elements*, Hunan Science & Technology Press: Changsha(in Chinese), 2001.
- [16] L. Chen and J. G. Huang, [Some error analysis on virtual element methods](#), *Calcolo*, **55** (2018), 23 pp.
- [17] L. Chen, H. Y. Wei and M. Wen, [An interface-fitted mesh generator and virtual element methods for elliptic interface problems](#), *J. Comput. Phys.*, **334** (2017), 327–348.
- [18] F. Feng, W. M. Han and J. G. Huang, [Virtual element method for an elliptic hmivariational inequality with applications to contact mechanics](#), *J. Sci. Comput.*, **81** (2019), 2388–2412.
- [19] F. Feng, W. M. Han and J. G. Huang, [Virtual element methods for elliptic variational inequalities of the second kind](#), *J. Sci. Comput.*, **80** (2019), 60–80.
- [20] A. L. Gain, C. Talischi and G. H. Paulino, [On the virtual element method for three-dimensional linear elasticity problems on arbitrary polyhedral meshes](#), *Comput. Methods Appl. Mech. Engrg.*, **282** (2014), 132–160.
- [21] J. J. Lai, J. G. Huang and C. M. Chen, [Vibration analysis of plane elasticity problems by the \$C^0\$ -continuous time stepping finite element method](#), *Appl. Numer. Math.*, **59** (2009), 905–919.

- [22] J. J. Lai, J. G. Huang and Z. C. Shi, [Vibration analysis for elastic multi-beam structures by the \$C^0\$ -continuous time-stepping finite element method](#), *Int. J. Numer. Methods Biomed. Eng.*, **26** (2010), 205–233.
- [23] I. Perugia, P. Pietra and A. Russo, [A plane wave virtual element method for the Helmholtz problem](#), *ESAIM Math. Model. Numer. Anal.*, **50** (2016), 783–808.
- [24] P.-A. Raviart and J.-M. Thomas, *Introduction à L'analyse Numérique des Équations aux Dérivées Partielles*, Collection Mathématiques Appliquées pour la Maîtrise, Masson, Paris, 1983.
- [25] O. J. Sutton, [The virtual element method in 50 lines of MATLAB](#), *Numer. Algorithms*, **75** (2017), 1141–1159.
- [26] C. Talischi, G. H. Paulino, A. Pereira and I. F. M. Menezes, [PolyMesher: A general-purpose mesh generator for polygonal elements written in Matlab](#), *Struct. Multidiscip. Optim.*, **45** (2012), 309–328.
- [27] G. Vacca, [Virtual element methods for hyperbolic problems on polygonal meshes](#), *Comput. Math. Appl.*, **74** (2017), 882–898.
- [28] G. Vacca and L. Beirão da Veiga, [Virtual element methods for parabolic problems on polygonal meshes](#), *Numer. Methods Partial Differential Equations*, **31** (2015), 2110–2134.
- [29] P. Wriggers, W. T. Rust and B. D. Reddy, [A virtual element method for contact](#), *Comput. Mech.*, **58** (2016), 1039–1050.
- [30] J. K. Zhao, S. C. Chen and B. Zhang, [The nonconforming virtual element method for plate bending problems](#), *Math. Models Methods Appl. Sci.*, **26** (2016), 1671–1687.
- [31] J. K. Zhao, B. Zhang, S. C. Chen and S. P. Mao, [The Morley-type virtual element for plate bending problems](#), *J. Sci. Comput.*, **76** (2018), 610–629.

Received February 2020; revised April 2020.

E-mail address: jghuang@sjtu.edu.cn

E-mail address: sjtu.Einsteinlin7@sjtu.edu.cn